On searches for gravitational waves from mini creation events by laser interferometric detectors

Bhim Prasad Sarmah[1,2], S.K. Banerjee[1,3], S.V. Dhurandhar[1] and J.V. Narlikar[1]
1. Inter-University Centre for Astronomy and Astrophysics, Post Bag 4, Ganeshkhind
Pune-411007, India
2. Department of Mathematical Sciences, Tezpur University
Tezpur-784028, India
3. Department of Mathematics, Amity School of Engineering, Sector-125
Noida-201301, India
E-mail : bhim@tezu.ernet.in, skb@iucaa.ernet.in, sanjeev@iucaa.ernet.in, jvn@iucaa.ernet.in

Abstract

As an alternative view to the standard big bang cosmology the quasi-steady state cosmology(QSSC) argues that the universe was not created in a single great explosion; it neither had a beginning nor will it ever come to an end. The creation of new matter in the universe is a regular feature occurring through finite explosive events. Each creation event is called a mini-bang or, a mini creation event(MCE). Gravitational waves are expected to be generated due to any anisotropy present in this process of creation. Mini creation event ejecting matter in two oppositely directed jets is thus a source of gravitational waves which can in principle be detected by laser interferometric detectors. In the present work we consider the gravitational waveforms propagated by linear jets and then estimate the response of laser interferometric detectors like LIGO and LISA.

Key words : cosmology: theory; mini creation; gravity waves

1 Introduction

The Quasi-Steady State Cosmology(QSSC) was proposed and explored in a series of papers by Hoyle et al(1993, 1994a,b, 1995) as a possible alternative to the standard big bang cosmology. The QSSC is based on a Machian theory of gravity which satisfies the Weyl postulate and the cosmological principle. The effective field equations are Einstein's equations of general relativity together with a negative cosmological constant and a trace-free zero mass scalar field which yield a wide range of solutions for the spatial sections of zero, positive and negative curvatures(Sachs et al 1996).

Instead of a single initial infinite explosion called the big bang, the QSSC has a universe without a beginning and its dynamical behaviour is sustained by an endless chain of mini-bangs better known as mini creation events(MCE) randomly distributed over space. The

universe itself has a longterm de-Sitter type expansion with a characteristic time scale of $\sim 10^{12}$ yrs, along with short term oscillations of period ~ 50 Gyrs. The oscillations respond in phase to 'on-off' creation activity in MCEs, with matter being created only in strong gravitational fields associated with dense aggregates of matter. The typical mini creation event may explain the outpouring of matter and radiation from a wide range of extragalactic objects of varying sizes ranging from superclusters-size mass $\sim 10^{16} M_{\odot}$ to masses of the order of 10^6-$10^{13} M_{\odot}$(Hoyle et al 1993). The cosmology has offered alternative interpretations of phenomena like the microwave background, abundances of light nuclei, the $m - z$ relation of high redshift supernovae, etc. (Hoyle, et al. 2000, Narlikar et al. 2002) and has also suggested tests to distinguish it from the standard model (Narlikar and Padmanabhan, 2001). One such possibility is provided by gravitational wave astronomy.

Gravational waves are expected to be generated if anisotropy is present in a mini creation event. Das Gupta and Narlikar(1993) had performed a preliminary calculation relating the size and anisotropy of a typical MCE to the feasibility of its being detected by LIGO type detectors. Here we carry out a more refined study of MCEs in which matter is ejected more like a jet. We must have a realistic model of the detector noise $n(t)$ to decide what information could be extracted from gravitational waveforms. This noise might have both Gaussian and non-Gaussian components but we will restrict ourselves to the statistical errors arising from Gaussian noise only. We can describe the remaining Gaussian noise by its spectral density $S_n(f)$, where f is the frequency. The form of $S_n(f)$ of course depends on the parameters of the detector.

We first consider the cosmogony of the creation process which leads to the creation and ejection of matter. We show why the creation phenomenon may have a non-isotropic character, with ejection taking place along preferred directions. To measure its gravitational wave effect we perform the calculation of gravitational amplitude generated by mini creation event of mass M at a cosmological distance r and then compare the signal to noise ratio (SNR) detectable by the ground based laser interferometric detector of the LIGO and the advance LIGO type within the frequency range of 10 Hz - 1000 Hz with the SNR detectable by the LISA-Laser Interferometric Space Antenna within the frequency range from 10^{-4} Hz to 10^{-1} Hz.

2 Matter Creation in the QSSC

The creation of matter in the QSSC proceeds via an exchange of energy from a background reservoir of a scalar field C of negative energy and stresses. The details of the process have been described in Hoyle et al (2000) and QSSC papers eg. Hoyle, et al. (1995), Sachs et al. (1996). We outline here the relevant aspects of the process that concerns us here.

First, the basic particle to be created is the so called Planck particle which has mass

$$m_p = \sqrt{\frac{3\hbar c}{4\pi G}}\,. \tag{1}$$

This particle itself is unstable on the time scale of 10^{-43} seconds. It subsequently decays into baryons through a series of processes that are currently discussed in the GUTs $\rightarrow$ Quark Gluon Plasma $\rightarrow$ Baryons in high energy particle physics. However, the initial stage of this sequence of events concerns us here, viz. the location of creation of Planck particles. Can creation take place anywhere? The answer is 'No'. The process requires a high enough energy threshold of the C - field:

$$C_i C^i = m_p^2 c^4, \tag{2}$$

where $C_i = \partial C/\partial x^i$, x^i $(i = 0, 1, 2, 3, x^0$ time like) being the spacetime co-ordinates.

The normal cosmological background of the C - field is below this threshold. Had the universe been homogeneous, there would have been no creation of matter. However, the real universe, although smooth and homogeneous on a large enough scale (so that it can be described by the Robertson - Walker line element), has pockets of strong gravitational field, such as in the neighbourhood of collapsed massive objects, often dignified by the name 'black holes'.

We shall use the name 'near black hole' (NBH) to denote a collapsed massive object whose size is very slightly in excess of that of its event horizon, *if it were a Schwarzschild black hole*. Thus a spherical object of mass M would have a radius

$$r_0 = \frac{2GM}{c^2} + \epsilon, \qquad \epsilon \ll r_0. \tag{3}$$

In the neighbourhood of such an object, at a distance r from its centre,

$$C_i C^i = \frac{{m_c}^2}{1 - \frac{2GM}{c^2 r}}, \qquad r > r_0\,, \tag{4}$$

where $m_c (< m_p)$ is the background level of the C - field energy density. It is thus possible that at r sufficiently close to r_0, the value of $C_i C^i$ crosses the creation threshold. This is when creation of matter would take place. And, because the creation of matter is accompanied by the creation of the C - field, the latter generates negative stresses close to $r = r_0$, which blow the created matter outwards.

In the above example the creation is isotropic and the resulting disturbances will not generate gravitational waves. This situation is, however, highly idealized. The real massive object will not be spherically symmetric, nor would the creation and expulsion of new matter from it be isotropic about its centre.

Even the next stage of asymmetry is sufficient to generate gravitational waves. namely that of a spinning collapsed massive object which is idealized as the Kerr black hole. The line element of the external spacetime for such a black hole is given by

$$ds^2 = \frac{\Delta}{\Sigma}(dt - h\sin^2\theta d\phi)^2 - \frac{\sin^2\theta}{\Sigma}[(r^2 + h^2)d\phi - hdt]^2 - \frac{\Sigma}{\Delta}dr^2 - \Sigma d\theta^2, \tag{5}$$

where

$$\Delta \equiv r^2 - 2mr + h^2, \quad \Sigma \equiv r^2 + h^2\cos^2\theta, \tag{6}$$

and $m = MG/c^2$, $h = J/Mc$ where, M and J are respectively the mass and angular momentum of the black hole. The Kerr black hole has an outer horizon at

$$r_+ = m + \sqrt{m^2 - h^2}, \tag{7}$$

while the surface of revolution given by,

$$r_s(\theta) = m + \sqrt{m^2 - h^2 \cos^2\theta}, \tag{8}$$

is called the static limit. Between r_+ and r_s is the region known as the ergosphere, wherein matter is made to rotate in the same direction as the spinning black hole.

As in the case of the Schwarzschild Black Hole the spinning collapsed massive object here will simulate a near black hole with spin and its exterior solution will be approximately given by the above equation (7). Here too we expect the $C_i C^i$ to be raised above the threshold close to the horizon. For, it is given by

$$C_i C^i = \frac{[(r^2 + h^2)(r^2 + h^2\cos^2\theta) + 2mrh^2\sin^2\theta]}{(r^2 + h^2\cos^2\theta)(r^2 - 2mr + h^2)}. \tag{9}$$

It can be seen that the above expression is maximum at poles ($\theta = 0, \pi$) and minimum at the equator ($\theta = \pi/2$). Thus the creation threshhold will be attained more easily at the poles than at the equator, leading to preferential creation of matter there. However, because of the ergosphere property of dragging any matter along with the spinning mass, only matter created near the polar regions ($\theta = 0, \pi$) would find it way out as it is ejected by the C - field. *In other words we expect created matter to find its way out along the polar directions in the form of oppositely directed jets.* This is the canonical source of gravitational waves in the QSSC.

A word of caution is needed in the above argument. We have assumed that in the neighbourhood of a typical NBH, the strength of the cosmological C - field will be small. Thus we have assumed that the Schwarzschild and Kerr solutions are not significantly modified by the C - field. This assumption can be checked only by obtaining an exact solution of a NBH with the C - field. We have not carried out this (rather difficult, possibly impossible) exercise; but have relied on approximations based on series expansions. In any case for the purpose of this paper, we have given a rationale for expecting the simplest cosmological sources of gravitational waves as twin jet systems spewing out newly created matter linearly in opposite directions.

3 Gravitational radiation from a mini creation event

In the QSSC the created matter near a Kerr-like black hole moves rapidly along the polar directions in the form of oppositely directed jets. Such an object is endowed with a changing quadrupole moment causing the system to emit gravitational waves. In the following we estimate its amplitude.

We set up a spherical polar co-ordinate system in which the jet is expanding linearly with a speed u in ϵ-ψ direction and consider the z-direction to be the line of sight. The gravitational wave amplitude under quadrupole approximation (a good approximation for a very long distance source) can be calculated from the reduced mass quadrupole moment of the source. The reduced mass quadrupole moment of a source is given by

$$Q_{ij} = \int_V \rho dV \left(r_i r_j - \frac{1}{3}\delta_{ij} r^2 \right), \tag{10}$$

where ρ is the mass per unit volume. We assume that away from the near black hole the geometry is almost Euclidean.

The components of gravitational wave amplitude at detector time t are given by

$$\bar{h}_{ij} = \frac{2G}{c^4 R} \left[\ddot{Q}_{ij} \left(t - \frac{R}{c} \right) \right], \tag{11}$$

where R is the radial distance of the object from the detector. At the source we have the time $t_0 = t - R/c$. The transverse traceless components can be extracted from $\bar{h}_{ij}$ through the projection operator $P^b_a = \delta^b_a - n^b n_a$ as

$$\bar{h}^{TT}_{ij} = P^k_i P^l_j \bar{h}_{kl} - \frac{1}{2} P_{ij} \left(P^{kl} \bar{h}_{kl} \right). \tag{12}$$

For gravitational waves propagating along z-direction, $n_a = (0, 0, 1)$, the '+' and the '$\times$' polarisation components of the wave are

$$h_+ = \frac{\bar{h}_{11} - \bar{h}_{22}}{2} \text{ and } h_\times = \bar{h}_{12}. \tag{13}$$

We will assume the radial velocity of the jet to be u so that $|ut_0| << R$.

For a time t_0 typical of the source, the three spatial co-ordinates are $r_1 = ut_0 \sin\epsilon \cos\psi$, $r_2 = ut_0 \sin\epsilon \sin\psi$ and $r_3 = ut_0 \cos\epsilon$. The non-vanishing components of the symmetric mass quadrupole moment (Q_{ij}) tensor are :

$$\begin{aligned}
Q_{11} &= \frac{2Q_0}{3} \left(\sin^2\epsilon \cos^2\psi - \frac{1}{3} \right), \\
Q_{12} &= \frac{Q_0}{3} \sin^2\epsilon \sin 2\psi, \\
Q_{13} &= \frac{Q_0}{3} \sin 2\epsilon \cos\psi, \\
Q_{22} &= \frac{2Q_0}{3} \left(\sin^2\epsilon \sin^2\psi - \frac{1}{3} \right), \\
Q_{23} &= \frac{Q_0}{3} \sin 2\epsilon \sin\psi, \\
Q_{33} &= \frac{2Q_0}{3} \left(\cos^2\epsilon - \frac{1}{3} \right),
\end{aligned} \tag{14}$$

where $Q_0 = \dot{M}u^2t_0^3$. The mass creation rate is $\dot{M} = A\rho u$, where A is the area of the jet.

The two polarisation components can be calculated as

$$\begin{aligned} h_+(t_0) &= h_{char}\sin^2\epsilon\cos 2\psi, \\ h_\times(t_0) &= h_{char}\sin^2\epsilon\sin 2\psi, \end{aligned} \tag{15}$$

where

$$\begin{aligned} h_{char} &= \frac{4G\rho A u^3 t_0}{c^4 R} = \frac{4G\dot{M}u^2 t_0}{c^4 R} \\ &\sim 2.7\times 10^{-17}\left(\frac{\dot{M}}{200\ M_\odot/\mathrm{sec}}\right)\left(\frac{u}{0.8c}\right)^2\left(\frac{t_0}{1000\ \mathrm{sec}}\right)\left(\frac{R}{3\ \mathrm{Gpc}}\right)^{-1}. \end{aligned} \tag{16}$$

The mini creation event sweeps over the band of the detector from high to low frequency. For LISA the low end of the band is taken to be 10^{-4} Hz which corresponds to about 10^4 sec $\sim$ few hours. In this period the LISA hardly changes orientation. Assuming random distribution and orientation of the MCE we perform appropriate averages over the directions and orientation of the MCE.

The angle averaging of a quantity V is performed according to

$$\begin{aligned} < V >_\psi &= \left[\frac{1}{2\pi}\int_0^{2\pi} V^2 d\psi\right]^{\frac{1}{2}}, \\ < V >_\epsilon &= \left[\frac{1}{2}\int_0^{\pi} V^2 \mathrm{sin}\epsilon \mathrm{d}\epsilon\right]^{\frac{1}{2}}, \\ < V >_{\epsilon,\psi} &= \left[\frac{1}{4\pi}\int_{\psi=0}^{2\pi}\int_{\epsilon=0}^{\pi} V^2 \mathrm{sin}\epsilon \mathrm{d}\epsilon \mathrm{d}\psi\right]^{\frac{1}{2}}. \end{aligned}$$

Thus,

$$\begin{aligned} < h_+(t_0) >_\psi &= < h_\times(t_0) >_\psi = \frac{1}{\sqrt{2}}\, h_{char}\sin^2\epsilon, \\ < h_+(t_0) >_{\epsilon,\psi} &= < h_\times(t_0) >_{\epsilon,\psi} = \frac{2}{\sqrt{15}}\, h_{char}. \end{aligned} \tag{17}$$

Before proceeding further we look at the overall stability of the system under the energy loss suffered through gravitational waves. An order of magnitude calculation indicates the situation as follows.

The rate of emission of gravitational waves corresponding to (16) above is given by

$$P_{GW} \cong \frac{c^3}{16\pi G}\alpha\left(\frac{4G\dot{M}u^2}{c^4 R}\right)^2 \times 4\pi R^2\,, \tag{18}$$

where α is a dimensionless constant of order unity (vide, for example, Misner, et al. 1973, p.975 - 1005). We compare this with the rate of addition of kinetic energy to the system

$$P_{KE} \cong \frac{1}{2}\dot{M}u^2. \tag{19}$$

If this ratio $P_{GW} : P_{KE}$ is small compared to unity, the radiation reaction will not slow down the source significantly. From (18) and (19) we get

$$\eta = \frac{P_{GW}}{P_{KE}} \cong \frac{8\alpha G\dot{M}u^2}{c^5} = 8\alpha\frac{G\dot{M}}{c^3}\beta^2\,, \tag{20}$$

where $u = \beta c$. (Although we have taken $\beta = 0.8$ as a typical example, the above Newtonian calculation will not give results too much different from the relativistic one within the order of magnitude.)

For $\dot{M} = 200M_\odot$ /sec, and $\alpha \sim 1$ we have, $\eta \sim 5 \times 10^{-3}$. In short, by this simple minded calculation, the kinetic energy created in the source well exceeds the energy radiated away. So by this argument we do not expect the source dynamics to be affected by the radiation process. However, a more detailed computation is required to determine the effect of radiation reaction. This we do not perform here since our goal in this investigation is to obtain only order of magnitude results.

Another aspect of the solution is whether the quadrupole moment formula used in (10) is sufficient to describe the scenario adequately. Had the speed of the jet been small compared to c, i.e., $\beta \ll 1$, we would have been certain of this. In the present case we have taken $\beta \sim 0.8$ and so the implications need a more careful attention. One notes in this case that higher order terms are extremely complex to calculate. Given the approximate nature of our source geometry such an exercise is not worth the effort. As we are, at this stage, interested in evaluating the order of magnitude of the overall effect we can argue as follows. For each extra order, the magnitude of the contribution is reduced by the factor β. Thus multipoles of higher order would contribute terms of the order β, β^2, β^3, etc., which do not significantly modify the estimate given by the first (quadrupole) term.

4 Fourier Transform of the gravitational wave amplitude

The two polarisations of gravitational wave amplitude that we have found in the earlier section have to be expressed in a limited frequency space within which the detector is supposed to be most sensitive. Also here we redefine our zero of time as the instant when the gravitational radiation first hits the observer.

The Fourier transform of $h_+(t_0)$ and $h_\times(t_0)$ are given by

$$\tilde{h}_+(f) \;=\; \int_{-\infty}^{\infty} h_+(t_0)\, exp\,(-2\,\pi\, i\, f\, t_0)\, dt_0$$

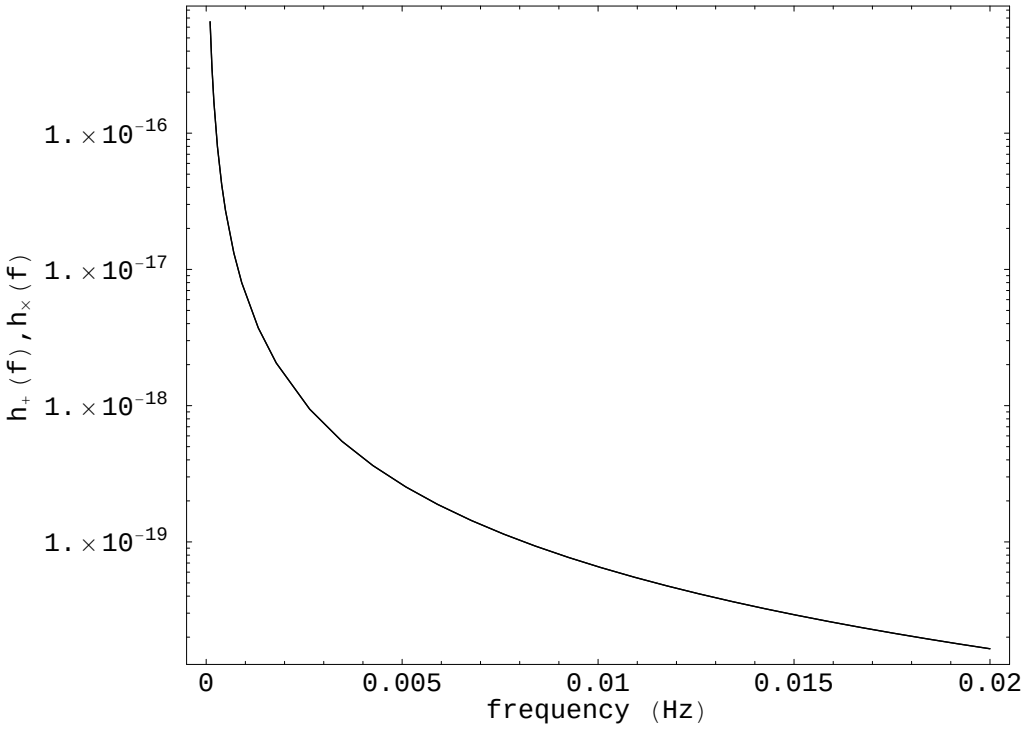

Figure 1: The Fourier Transform of the two polarisations of the wave in units of Hz^{-1} are plotted here as a function of frequency for a MCE jet with $\dot{M} = 200 M_\odot$ /sec, $R = c/2H_0$ (for $h_0 = 0.65$), $u = 0.8c$. Here $\epsilon \sim 15^0$ and ψ is averaged over uniformly. The two components thus averaged are of the same amplitude and hence they overlap.

$$= \frac{\dot{M}Gu^2}{\pi^2 c^4 R}\frac{1}{f^2}\sin^2\epsilon\cos 2\psi. \tag{21}$$

$$\tilde{h}_\times(f) = \int_{-\infty}^{\infty} h_\times(t_0)\, exp(-2\pi\, i\, f\, t_0)\, dt_0$$

$$= \frac{\dot{M}Gu^2}{\pi^2 c^4 R}\frac{1}{f^2}\sin^2\epsilon\sin 2\psi. \tag{22}$$

Plots of $\tilde{h}_+(f)$ and $\tilde{h}_\times(f)$ are shown in Figure 1. Since the frequency f appears in the denominators of the above expressions, the amplitude of the jet falls in inverse square fashion as it expands. This causes most of the wave energy to be concentrated in the low frequency bin. It is thus worthwhile to analyse the detectibility of such a wave through low frequency detector such as LISA. We will also compare the results with the magnitude detectable by the high frequency detector like LIGO.

The $1/f^2$ dependence might suggest infrared divergence of this formula as $f \to 0$. However, the assumed geometry and lifetime of expansion of the source is finite, i.e., t_0 is bounded

above. At the relativistic speed assumed here, the source would attain a size of ~ 200 kpc in a time of $\sim 10^6$ yrs. If the source slows down, the time scale may be longer, typically $\sim 10^8$ yrs. Thus instead of $f \to 0$ we have f bounded below, and no divergence arises.

5 Detectibility of MCE by LISA capability

5.1 Time Delay Interferometry of LISA

LISA, the Laser Interferometric Space Antenna, is a proposed mission that will use coherent laser beams exchanged between three identical spacecraft forming a giant equilateral triangle with each side 5×10^6 km to observe and detect low frequency gravitational waves from cosmic sources.

In LISA six data streams arise from the exchange of laser beams between the three spacecraft. The sensitivity of LISA crucially depends on the cancellation of the laser frequency noise. It is because of the impossibility to achieve equal distances between spacecraft, the laser frequency cannot be exactly cancelled to enhance its sensitivity. Several schemes came up to combine the recorded data with suitable time delays corresponding to the three arm lengths of the giant triangular interferometer.

The idea of time delayed data combination scheme was proposed by the Jet Propulsion Laboratory team (1999a, 1999b, 2000). Dhurandhar et. al.(2002) adopted an algebraic approach to this problem of introducing time delays to cancel the laser frequency noise based on the modules over polynomial rings.

The data combinations that cancel the laser frequency noise consist of six suitably delayed data streams, the delays being integer multiples of the light travel times between spacecraft, which can be conveniently expressed in terms of polynomials in the three delay operators E_1, E_2, E_3 corresponding to the light travel time along the three arms. The laser noise cancellation condition puts three constraints on the six polynomials of the delay operators corresponding to the six data streams. The problem therefore consists of finding six-tuples of polynomials that satisfy the laser noise cancellation constraints. These polynomial tuples form a module, called the *module of syzygies*.

Given any elementary data streams U^i, V^i, a general data combination is a linear combination of these elementary data streams

$$X(t) = \sum_{i=1}^{3} p_i V^i(t) + q_i U^i(t)\,, \tag{23}$$

where p_i and q_i are polynomials in the time-delay operators $E_i,\ i = 1, 2, 3$. Thus any data combination can be expressed as a six-tuple polynomial 'vector' (p_i,q_i). For cancellation of laser frequency noise only the polynomial vectors satisfying this constraint are allowed and they form the module of syzygies mentioned above. While the laser frequency noise and optical bench motion noise can be canceled by taking appropriate combinations of the beams in

the module of syzygies, the acceleration noise of the proof masses and the shot noise cannot be canceled out in the scheme. These then form the bulk of the noise spectrum. The noise power spectral density is also expressible in terms of the noise cancelling polynomials of the time delay operators. For different combinations, the expression for the noise spectrum will also be different.

In our analysis we use the Michelson combination to calculate the response and the noise power spectral density. As shown in Nayak et. al. (2003), the Michelson combination on the average has almost as good sensitivity as the optimized combinations. Since here we are interested in order of magnitude estimates, the Michelson combination is good enough for our purpose. Moreover, it is easier to calculate relevant quantities for the Michelson combination than for other combinations.

5.2 Estimation of Signal-to-Noise Ratio of jets in LISA

We choose a co-ordinate system in which the LISA configuration is at rest and let x-axis of the co-ordinate system be perpendicular to one of the LISA arm unit vectors $(\hat{n}_1, \hat{n}_2, \hat{n}_3)$. The z-axis is considered perpendicular to the plane of the LISA triangle. The unit vector $\hat{w}$ connecting the origin and the source is parametrized by the source angular location (θ, ϕ), so that

$$\hat{w} = \begin{pmatrix} \sin\theta\,\cos\phi \\ \sin\theta\,\sin\phi \\ \cos\theta \end{pmatrix} \tag{24}$$

and the transverse plane is spanned by the unit transverse vector $\hat{\theta}$ and $\hat{\phi}$, defined by

$$\hat{\theta} = \frac{\partial\hat{w}}{\partial\theta}\ , \qquad \hat{\phi} = \frac{1}{\sin\theta}\frac{\partial\hat{w}}{\partial\phi}\ . \tag{25}$$

For the Michelson combination we have the following expressions of the polynomials:

$$\begin{aligned} p_i &= \{1 - E_2^2, 0, E_2(E_3^2 - 1)\}\,, \\ q_i &= \{1 - E_3^2, E_3(E_2^2 - 1), 0\}\,. \end{aligned} \tag{26}$$

In the Fourier domain, $E_i = e^{i\Omega L_i}$ where $\Omega = 2\pi f$ is the angular frequency. The LISA arm vectors are given by $\vec{r}_i = L_i\ \hat{n}_i$ $(i = 1, 2, 3)$. However, for purpose of calculation of the noise and response it is sufficient to consider all the L_i to be equal, to L say.

The noise power spectral density as given by Bender et. al. (2000) for this combination is

$$S_M = 16\ S_{shot}\ \sin^2 2\pi f L + S_{proof}(32\sin^2 2\pi f L + 8\sin^2 4\pi f L), \tag{27}$$

where,

$$\begin{aligned} S_{shot} &= 5.3 \times 10^{-38} f^2\ \mathrm{Hz}^{-1}\ , \\ S_{proof} &= 2.5 \times 10^{-48} f^{-2}\ \mathrm{Hz}^{-1}\ . \end{aligned}$$

Plot of the noise power density S_M for Michelson combination is shown in Figure 2. Several sets of generators have been listed in Dhurandhar et. al. (2002). The response of LISA to a source is expressible for a given data combination X in terms of its elementary data stream U^i, V^i as the following :

$$\mathcal{R}_X(\Omega;\theta,\phi,\epsilon,\psi) = \tilde{h}_+(\Omega;\epsilon,\psi)F_+(\Omega;\theta,\phi) + \tilde{h}_\times(\Omega;\epsilon,\psi)F_\times(\Omega;\theta,\phi) \tag{28}$$

where $F_{+,\times}(\Omega)$ are transfer functions which correspond to the combination X. These are functions of the source angular location and the frequency. For different noise cancelling combinations $U_i, V_i, F_{+,\times}(\Omega)$ will have different expressions. Below are quantities for U_1, V_1 (the others are obtained by cyclic permutations) :

$$\begin{aligned} F_{U_1;+,\times} &= \frac{e^{i\Omega(\hat{w}.\vec{r}_3+L_2)}}{2(1+\hat{w}.\hat{n}_2)} \times (1 - e^{-i\Omega L_2(1+\hat{w}.\hat{n}_2)})\xi_{2;+,\times} \ , \\ F_{V_1;+,\times} &= -\frac{e^{i\Omega(\hat{w}.\vec{r}_2+L_3)}}{2(1-\hat{w}.\hat{n}_3)} \times (1 - e^{-i\Omega L_3(1-\hat{w}.\hat{n}_3)})\xi_{3;+,\times} \ , \end{aligned} \tag{29}$$

where,

$$\begin{aligned} \xi_{i;+} &= (\hat{\theta}.\hat{n}_i)^2 - (\hat{\phi}.\hat{n}_i)^2 \ , \\ \xi_{i;\times} &= 2(\hat{\theta}.\hat{n}_i)(\hat{\phi}.\hat{n}_i). \end{aligned} \tag{30}$$

In the above L_i are LISA arm lengths (i=1,2,3), $\hat{w}$ is the unit vector along the line of sight, $\hat{\theta}$ and $\hat{\phi}$ are the unit vectors transverse to the line of sight.

The response of LISA to Michelson combination is given by

$$\mathcal{R}_M = \sum_{i=1}^{3}[p_i(F_{Vi;+}h_+ + F_{Vi;\times}h_\times) + q_i(F_{Ui;+}h_+ + F_{Ui;\times}h_\times)] \ , \tag{31}$$

where the polynomial functions p_i and q_i are for the Michelson combination given in equation (26). The signal-to-noise ratio corresponding to a particular frequency, say f, is given by

$$SNR_f = \frac{|\mathcal{R}_M|}{\sqrt{S_M}}. \tag{32}$$

The integrated signal-to-noise ratio is then given by

$$SNR = \left[2\int_0^\infty \frac{|\mathcal{R}_M|^2}{S_M}\ df\right]^{\frac{1}{2}}. \tag{33}$$

The response $\mathcal{R}_M$ is now a function of $\epsilon, \psi, \theta, \phi$ and the frequency f. Since the detector is omnidirectional, it will pick up all such sources of various orientations and frequencies in its response. So, one needs to average the response over the orientations of the source and the detector. The expression for the integrated SNR takes care of the frequency averaging.

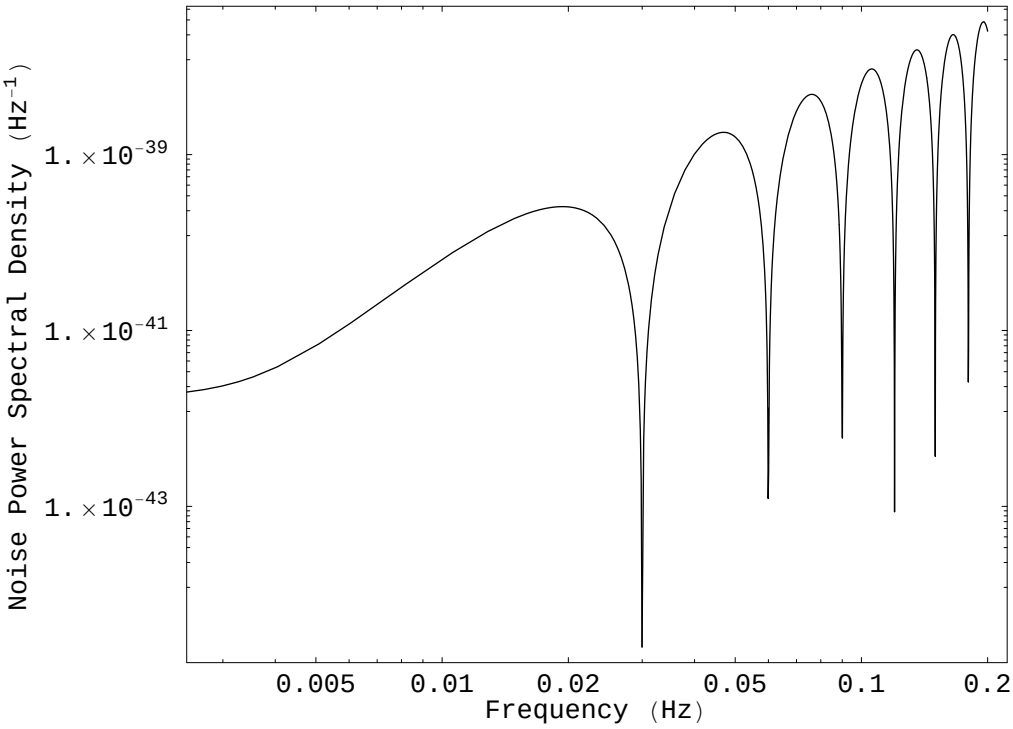

Figure 2: Noise power spectral density S_M for Michelson combination, as a function of frequency.

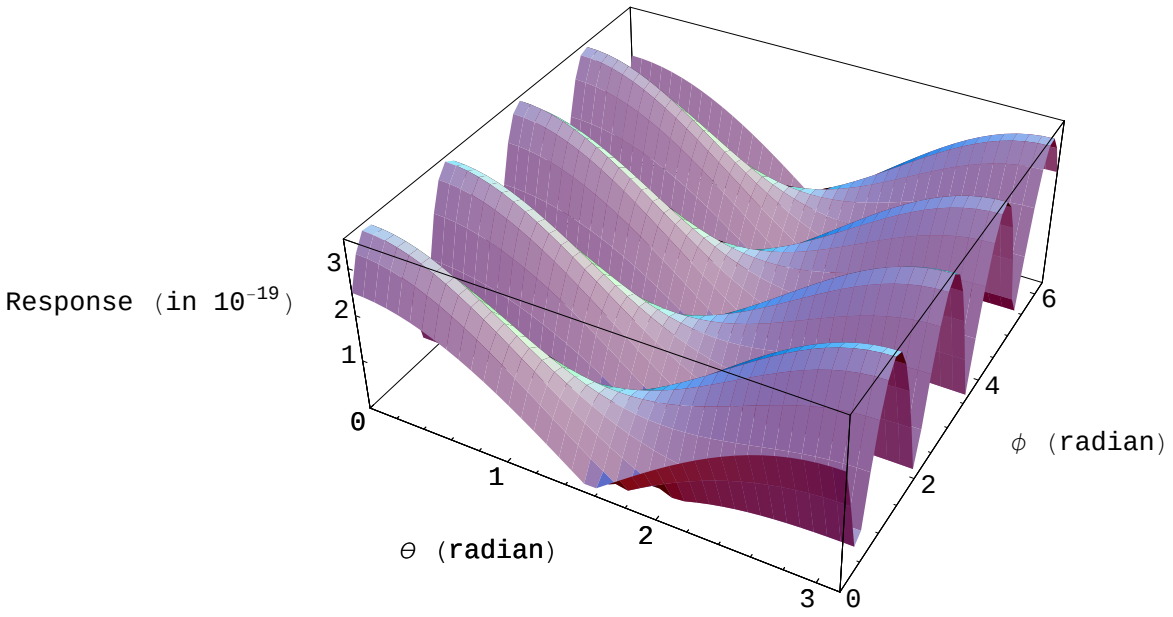

Figure 3: Response $\mathcal{R}_M$ of LISA to the jet source at $f = 1$ mHz as function of angular location (θ, ϕ) of the source for the Michelson combination.

We apply this model to a superluminal jet beaming towards us nearly at an angle 15^o from a distance of about half the Hubble distance and with a speed of nearly 80% of the speed of light in vacuum, i.e. in this case, $u = 0.8c$, $\epsilon = 15^o$, $R = c/2H_0$ (for $h_0 = 0.65$).

Plot of $\mathcal{R}_M$ of LISA for the Michelson combination is shown in Figure 3. We have implemented the response function given by Dhurandhar et al. (2002) and their proper angle averaging and calculated the signal-to-noise-ratio as a function of frequency and the integrated signal-to-noise ratio over the frequencies in the LISA window. Because the sensitivity of LISA window starts 'bumping' in the higher frequency side, and also because the jet source has comparatively lower amplitude in this region and thus contributes less to the integrated signal-to-noise ratio, we consider a frequency range 10^{-4} Hz - 2×10^{-2} Hz for LISA sensitivity to calculate the relevant quantities.

We therefore compute the suitably averaged SNR for the source at about 3 Gpc. It is apparent that the SNR scales linearly with the mass creation rate as follows:

$$SNR = 5.19 \times \left(\frac{\dot{M}}{100\ M_\odot/\mathrm{sec}} \right). \tag{34}$$

This is also obvious from the expression for the gravitational wave amplitude. From this expression, the minimal mass creation rate for which a source is just observable, can be calculated. Here we consider this 'bare visibility' value for SNR to be 10. In this case the mass creation rate turns out to be about $200 M_\odot$/sec.

Although it is easier to compute the SNR using only the instrumental noise, a remark is in order here, because the instrumental noise in LISA below 1 mHz is dominated by the 'confusion' noise from galactic binaries. These independent unresolved sources form a stochastic background which stands above the instrumental noise. Since Eq. [34] only takes into account the instrumental noise in LISA, the SNR as calculated above will degrade because the confusion noise will effectively raise the noise floor at low frequencies. A recent calculation has been performed by Edlund et al (2005) of the galactic background noise which shows that the previous estimates of this noise were over estimates and the level of the noise is a factor of 2 or more less than was previously thought. Using this current result, we estimate that the SNR given in Eq. [34] will be degraded by less than 10 % on account of the galactic confusion noise. This then does not affect our order of magnitude estimate of the SNR.

The net gravitational wave amplitude from an MCE, in the linear approximation, can be thought of as arising from the superposition of gravitational waves from individual fluid elements of the MCE. If f is the frequency of interest, coherent superposition of amplitudes occurs only from within a region $2\mathcal{L}$ of size less than $0.5\lambda = 0.5c/f$. For the LISA window ($f_1 = 10^{-4}$ – $f_2 = 2 \times 10^{-2}$) Hz, we have

$$2\mathcal{L}_1 < \frac{c}{2 \times 10^{-4}\ \mathrm{Hz}} \qquad \Rightarrow \qquad \mathcal{L}_1 < (2500\ \mathrm{seconds}) \times \mathrm{c}$$
$$2\mathcal{L}_2 < \frac{c}{2 \times 2\ 10^{-2}\ \mathrm{Hz}} \qquad \Rightarrow \qquad \mathcal{L}_2 < (12.5\ \mathrm{seconds}) \times \mathrm{c}$$

i.e., towards higher frequency side the jet length limit is smaller and towards lower, it is larger. This means, under the linear approximation, the gravitational wave frequency in LISA window will carry information about the MCE during which jet acquires the above length limit. This length limit can be converted to time limit from the knowledge of the velocity of expansion of the jets. The corresponding time limit is:

$$\left(\frac{\mathcal{L}_1}{u} - \frac{\mathcal{L}_2}{u}\right) = \left(\frac{2500c}{0.8c} - \frac{12.5c}{0.8c}\right) \text{ seconds } \simeq 3100 \text{ seconds} \approx 52 \text{ minutes},$$

i.e., LISA observation of MCE can look into the history from 15 seconds after the birth of an MCE for a duration of about 52 minutes. But LISA will be able to 'see' the jets for which the mass creation rate is at least $\dot{M} = 200 M_\odot$/sec. This mass creation rate then gets converted to a single jet mass window of $(1.56 \times 10^3,\ \ 3.13 \times 10^5)\, M_\odot$/sec.

6 Observation of MCE by LIGO type detector

For the LIGO type detectors Wiener optimal filters $q(t)$ are used. These filters are defined by their Fourier transform(Thorne 1987, Schutz 1991) as

$$\tilde{q}(f) = k\frac{\tilde{h}(f)}{S_n(f)}, \tag{35}$$

where $S_n(f)$ is the power spectral density of the noise in the detector and k is a normalisation constant. For a laser interferometric detector of advance LIGO type $S_n(f)$ is given in the following form:

$$S_n(f) = \begin{cases} \infty, & f \ < \ 10 \text{ Hz}, \\ S_0[(\frac{f_0}{f})^4 + 2\{1 + (\frac{f^2}{{f_0}^2})\}], & f \ > \ 10 \text{ Hz}, \end{cases} \tag{36}$$

where $S_0 = 3 \times 10^{-48} \text{Hz}^{-1}$ and $f_0 = 70$ Hz (Cutler and Flanagan, 1994 [1]). The amount of detector noise determines the strength of the weakest detectable signal by the detector. For a perfect frequency matching of the filters with the signal, the cross-correlation between the detector outputs and the filter leads to a signal to noise ratio

$$\frac{S}{N} = \left[2\int_0^\infty \frac{|\bar{h}(f)|^2}{S_n(f)} df\right]^{1/2}. \tag{37}$$

We assume that the present detector is uniformly sensitive in the frequency band $f_l = 10$ Hz to $f_u = 1000$ Hz and is blind everywhere outside it. Then equation(16) reduces to the form

$$\frac{S}{N} = \frac{\sqrt{2} G\dot{M} u^2 f_0}{3c^4\pi^2 R {S_0}^{1/2}} \left[\int_{f_l}^{f_u} \frac{df}{(2f^6 + 2f_0^2 f^4 + f_0^6)}\right]^{1/2}, \tag{38}$$

Computing the integral numerically, we obtain,

$$\frac{S}{N} \sim \frac{G\dot{M}u^2}{c^4\pi^2 R}(3.76 \times 10^{20}) \text{ Hz}^{-1}. \tag{39}$$

[1]Since we are only interested in the order of magnitude estimated, this noise curve suffices.

On choosing the following values :

$$\begin{aligned} r &= \frac{c}{2H_0} \equiv \text{half the Hubble distance (for } h_0 = 0.65), \\ u &= \frac{8c}{10} \equiv \text{ eight tenth of the velocity of light,} \\ \dot{M} &= \frac{\kappa}{\tau} M_\odot, \ \kappa \text{ is a constant and } \tau \text{ is the proper time measured in seconds.} \end{aligned} \tag{40}$$

We obtain the following result:

$$\begin{aligned} \frac{S}{N} &\sim 5.3 \times 10^{-4} \left(\frac{\dot{M}}{M_\odot} \right) \\ &= 5.3 \times 10^{-4} \left(\frac{\kappa}{\tau} \right). \end{aligned} \tag{41}$$

We next relate such values to actual situations, for which we need to go back to the astrophysics of a mini-creation event. We return to Section 2 to discuss further details of the typical mini-creation event (MCE). The C-field obeys the wave equation with sources in the world points where particle creation takes place (Hoyle, et al 1995). So when matter is created at a point, the negative energy C-field tends to escape outwards more efficiently than the matter created, which has non-zero rest-mass. Thus initially the mass created adds to the existing massive object. It is this tendency that leads to build up of massive concentrations of matter such as found in the nuclei of galaxies. However, as the central mass grows and its gravitational field increases in strength, the free escape of the C-field quanta is inhibited and this leads to a concentration of the field in the object. Since the field has negative stress, the interior of the collapsed object tends to become unstable. With sufficient accumulation of C-field strength, it may break up and cause some pieces to be thrown out with great speed. It was this scenario that was envisaged in Section 2 and as stated there, if the collapsed object is a near-Kerr black hole, it will eject material along the axis. Although the material is coming out of a region of high gravitational red shift, its ejection speed can be even more dominant and allow it to come out with high speed. The situation is somewhat like the classical white hole (see for example Narlikar, et al 1974), except that in this case the C-field is the driving agent which prevents the outgoing material from being swamped out by the relative inward motion of the surrounding material, thus overcoming an objection to white holes envisaged by Eardley (1974). In such a case, the early expansion is very rapid, with the external observer receiving radiation that is highly blue shifted. The blue shift does not last long, however, and the expansion slows down subsequently.

Finally we address an important issue relating to the expected frequency of these events. If mass concentrations in the universe are too frequent, then there may be a confusion background of such events, making it impossible to detect single sources. If we confine our attention to radio sources, we may estimate their total number out to 3 Gpc to be about few times 10^8; this is the distance to which the SNR ~ 10 on the average or greater. This number can be arrived at by taking one radio galaxy per 100 Mpc^3 or one per few hundred Mpc^3. A characteristic time scale for a source is $\sim 10^8$ years. However, as we

have seen, the present specifications of the LISA detector allow observation of a source for a typical time-window of $\sim 3 \times 10^3$ sec. The chance of observing a given source is therefore 3×10^3 sec/10^8 yr $\sim 10^{-12}$. The total probability is therefore few times $10^8 \times 10^{-12} \sim$ few times 10^{-4}. Thus the observation in a characteristic time-window is a fairly rare one and certainly not one to generate noise. Given that there are $3 \times 10^7/3 \times 10^3 \sim 10^4$ such windows per year, we expect one to few positive detections by LISA over a year. We would like to point out here that these numbers are only approximate, because a detailed calculation should take into account effects such as the non-Euclidean nature of the specific cosmological model, etc. But nevertheless the numbers indicate that MCEs could be detected by LISA during its mission period.

7 Conclusions

The gravitational waves could be generated in a chain of endless mini bangs if there is a small anisotropy present in the process. An anisotropic mini creation event is the biggest source of the gravitational waves. The calculations we performed here show that a laser interferometric detector of the LISA type can be used to detect through a window of low frequency range 10^{-4} Hz to 2×10^{-2} Hz for a duration of about 52 minutes. In this duration LISA will be able see 'jets' for which the mass creation rate is at least 200 $M_\odot$/sec. Whereas a laser interferometric detector of the advance LIGO type can be used to detect the mini creation events, which opens its window of high frequency range 10 Hz to 10^3 Hz for a very short duration of the order of 10^{-2} seconds and in this duration it observes 'jets' for which the mass creation rate is 2×10^4 $M_\odot$/sec. It appears from this elementary analysis that the LISA detector is well suited to detect MCEs through their gravitational waves while the LIGO may have a less sensitive, marginal role to play.

References

Armstrong J.W., Eastabrook F. B., Tinto M., 1994, ApJ, 527, 814.

Bender P.*et al.*, 2000, 'LISA: A Cornerstone Mission for the Observation of Gravitational Waves', System and Technology Study Report ESA-SCI (2000), 11.

Bondi H., Gold T., 1948, MNRAS 108, 252.

Cutler C., Flanagan E. E., 1994, Phys. Rev. D 49, 2658.

Das Gupta P., Narlikar J. V., 1993, MNRAS 264, 489.

Dhurandhar S. V., Nayak K. Rajesh, Vinet J-Y., 2002, Phys. Rev. D 65, 102002.

Eardley, D.M. 1974, preprint.

Eastabrook F. B., Tinto M., Armstrong J.W., 2000, Phys. Rev. D 62, 042002.

Edlund J. A., Tinto M., Krolak A., Nelemans G., 2005, Phys. Rev. D 71, 122003.

Hoyle F., 1948, MNRAS 108, 372.

Hoyle F., Burbidge G., Narlikar J. V., 1993, ApJ 410, 437.

Hoyle F., Burbidge G., Narlikar J. V., 1994a, MNRAS 267, 1007.

Hoyle F., Burbidge G., Narlikar J. V., 1994b, A&A 289, 729.

Hoyle F., Burbidge G., Narlikar J. V., 1995a, Proc. Roy. Soc. A 448, 191.

Hoyle F., Burbidge G., Narlikar J. V., 2000, 'A Different Approach to Cosmology', Cambridge

Univ. Press, Cambridge.
Misner, C.W., Thorne, K. and Wheeler, J.A. 1973, *Gravitation*, W.H. Freeman and Company, New York..
Narlikar J.V., Apparao, K.M.V., Dadhich, N.K., 1974, Nature, 251, 590.
Narlikar J.V., Padmanabhan T, 2001, Annu. Rev. A&A, 39, 211.
Narlikar J.V., Vishwakarma R.G., Burbidge G., 2002, PASP, 114,1092.
Nayak K. Rajesh, Dhurandhar S.V., Pai A., Vinet J-Y., 2003, Phys. Rev. D 68, 122001.
Sachs R., Narlikar J. V., Hoyle F., 1996, A&A 313, 703.
Schutz B. F., 1991, in Blair D. G., ed., The Detection of Gravitational Waves. Cambridge Univ. Press, Cambridge, p. 406.
Thorne K. S., 1987, in Hawking S., Israel W., eds., 300 Years of Gravitation. Cambridge Univ. Press, Cambridge, p. 330.
Tinto M., Armstrong J.W., 1999, Phys. Rev. D 59, 102003.